Supplemental Materials for

Spin and dipole order in geometrically frustrated mixed-valence manganite $Pb_3Mn_7O_{15}$

S. A. Ivanov[a,b], A. A. Bush[c], M. Hudl[d], A. I. Stash[a], G. André[e], R. Tellgren[f], V. M. Cherepanov[g], A. V. Stepanov[c], K. E. Kamentsev[c], Y. Tokunaga[h], Y. Taguchi[h], Y. Tokura[h,i], P. Nordblad[b], and R. Mathieu[b]

a- Center of Materials Science, Karpov Institute of Physical Chemistry, Vorontsovo pole, 10 105064, Moscow, Russia
b- Department of Engineering Sciences, Uppsala University, Box 534, SE-751 21 Uppsala, Sweden
c- Moscow Technological University, RU-119434, Moscow, Russia
d- Department of Physics, Stockholm University, SE-106 91 Stockholm, Sweden
e- Laboratoire Leon Brillouin, CEA, Saclay, France
f- Department of Chemistry – Ångström Laboratory, Uppsala University, Box 538, SE-751 21 Uppsala, Sweden
g- National Research Centre "Kurchatov Institute", 123182 Moscow, Russia
h- RIKEN Center for Emergent Matter Science (CEMS), Wako 351-0198, Japan
i- Department of Applied Physics, University of Tokyo, Tokyo 113-8656, Japan

Contents

1. Experimental details

Chemical composition

The chemical composition of the prepared crystals of $Pb_3Mn_7O_{15}$ (PMO) was analyzed by energy-dispersive spectroscopy (EDS) using a JEOL 840A scanning electron microscope and INCA 4.07 (Oxford Instruments) software. The analyses performed on several domains showed that the concentration ratio of Pb/Mn is the stoichiometric one within the instrumental resolution (0.05).

Second harmonic generation (SHG) measurements.

The crystals were characterized by SHG measurements in reflection geometry, using a pulsed Nd:YAG laser. λ=1.064 μm). The SHG signal $I_{2\omega}$ was measured from the polycrystalline samples relative to α-quartz standard at room temperature in the Q-switching mode with a repetition rate of 4 Hz. To make relevant comparisons of PMO microcrystalline powders and α-quartz standard were sieved into the same particle size range because the SHG efficiency has been shown to depend strongly on particle size.

Single-Crystal X-ray diffraction (XRD)

A suitable black plate-shaped single crystal of PMO (0.04 × 0.11 × 0.014 mm) was selected for XRD analysis. No signs of twinning were observed. Integrated intensity data were collected on an Enraf-Nonius CAD-4 diffractometer with Mo Kα (λ = 0.71073 Å; β filter) radiation using the ω–2θ scan mode at room temperature. The scan speed and time for each reflection were varied so as to obtain $\sigma_I/I = 0.01$. The unit cell was determined from a least-squares fit to positions of 25 high-2θ reflections. The ranges of *hkl* values measured are $-12 < \boldsymbol{h} < 12$, $-12 < \boldsymbol{k} < 11$, and $0 < \boldsymbol{l} < 16$, giving a total number of measured reflections of 3579. Three standard reflections were measured every 60 min during data collection.

Out of the measured 424 independent reflections, there were 353 for which $I_{obs} > 2\sigma(I)$ and that could be used for refinement. Four standard reflections were measured; the variation in $I_{obs}$was around 1%. Each reflection was centered at eight different equivalent positions. The intensities were corrected for Lorentz–polarization effects and subsequently for absorption using the *PLATON-ABSGAUSS* program[1]. The structures were solved by direct methods and refined on F^2 with full-matrix least-squares methods using the *SHELXS-97* and *SHELXL-97* programs, respectively [2]. Scattering factors and anomalous dispersion terms for Pb, Mn and O were taken from Ref. [3]. The Pb and Mn atoms were first located, and the O atoms were found subsequently in the difference Fourier maps.

X-ray powder diffraction

Powder sample prepared from small crystals was checked from X-ray powder diffraction (XRPD) patterns obtained with a D-5000 diffractometer using Cu K_α radiation. Crystals were crushed into powder in an agate mortar and suspended in ethanol. Si substrate was covered with several drops of the resulting suspension, leaving randomly oriented crystallites after drying. The XRPD data for Rietveld analysis were collected at room temperature on a Bruker D8 Advance diffractometer (Ge monochromatized Cu $K_{\alpha 1}$ radiation, Bragg-Brentano geometry, DIFFRACT plus software) in the 2θ range 10-152° with a step size of 0.02° (counting time was 15 s per step). The slit system was selected to ensure that the X-ray beam was completely within the sample for all 2θ angles.

Neutron powder diffraction

Because the neutron scattering lengths of Pb and Mn are different, the chemical composition of these cations can be observed by neutron powder diffraction (NPD) with good precision, particularly for Pb and Mn because of opposite signs of their scattering factors(b_{Pb}= 9.405 , b_{Mn} = -3.73). The neutron scattering length of oxygen (b_O = 5.805 fm) is comparable to those of the heavy atoms and NPD provides accurate information on its position and stoichiometry.

Two sets of NPD data were collected on the sample and with different emphasis.Registration of NPD patterns versus temperature was performed at LLB (Saclay, France) on the high-resolution neutron powder diffractometer 3T2 (λ=1.225 Å) at different temperatures. The powdered sample (around 3 gr.) was inserted in a cylindrical vanadium container and a helium cryostat was used to collect data at several decisive temperatures in the temperature range 5-295 K and used for the main crystallographic refinements. The second set of powder patterns was obtained on the G 4-1 diffractometer at LLB. This diffractometer is equipped with a pyrolitic graphite monochromator and a linear multidetector composed of 800 cells (BF3) separated by 0.1° covering an angular range of 80° (2θ). The incident wavelength was λ = 2.426Å. The NPD data were collected at low temperatures down to 1.8 K using a standard He cryostat and with much finer temperature steps to follow the magnetic phase transitions. Nuclear and magnetic refinements were performed by the Rietveld method using the FULLPROF software [4]. The diffraction peaks were described by a pseudo-Voigt profile function, with a Lorentzian contribution to the Gaussian peak shape. A peak asymmetry correction was made for angles below 35° (2θ). Background intensities were estimated by interpolating between up to 40 selected points (low temperature NPD experimental data) or described by a polynomial with six coefficients. An analysis of coordination polyhedra of cations was performed using the IVTON software [5]. The magnetic propagation vector was determined from the peak positions of the magnetic diffraction lines using the K-search software which is included in the FULLPROF refinement package [4]. Magnetic symmetry analysis was then done using the program BASIREPS [4]. The different allowed models for the magnetic structure were one by one tested against the measured data. Each structural model was refined to convergence, with the best result selected on the basis of agreement factors and stability of the refinement

2. Thermogravimetry results

In addition to single crystals usual ceramic technology was used for a preparation of polycrystalline samples of PMO for Thermogravimetric analysis (TGA) to increase the amount of material and thus measurement accuracy. The temperature and duration of the first and second firing were 950 and 980 °C respectively. All registered XRPD reflections from ceramic sample were indexed on the basis of the hexagonal cell with a =9.9937 (5) and c =13.578 Å. No extra peaks were found which allows to conclude that ceramic sample was single-phase (with accuracy up to a sensitivity of our experimental set up).

Thermogravimetric research was performed on the ceramic samples of PMO at air atmosphere using automated derivatograph Q D 1500 system Paulik-Erdei. The results are shown in Figure SM1. In accordance with the data in Ref. [6] the PMO phase melts at 1020° C with decomposition into Mn_3O_4 and fluid. With increasing temperature from room temperature to 870° C sample mass almost does not change, indicating the stability of phase in this temperature range. Estimation of Δm(O) at 965° C allows to determine the amount of the reduction of oxygen index for phase $Pb_3Mn_7O_{15-x}$, which at this temperature equals Δx=0.36.

With further heating of the sample mass decreases, the speed of which increases with temperature. When cooling the sample mass increases again, but recovers only a portion of the mass loss that occurred in the previous heating.

Thus, the TGA investigation shows that during of heating above 870° C the oxygen content of PMO decreases, which at 965° C is around 0.36 oxygen atoms in the unit $Pb_3Mn_7O_{15}$ formula. This decrease is restoring when the sample cools, but after quenching with high temperatures it can be stored at room temperature, especially reflecting on crystal structure and physical properties of crystals.

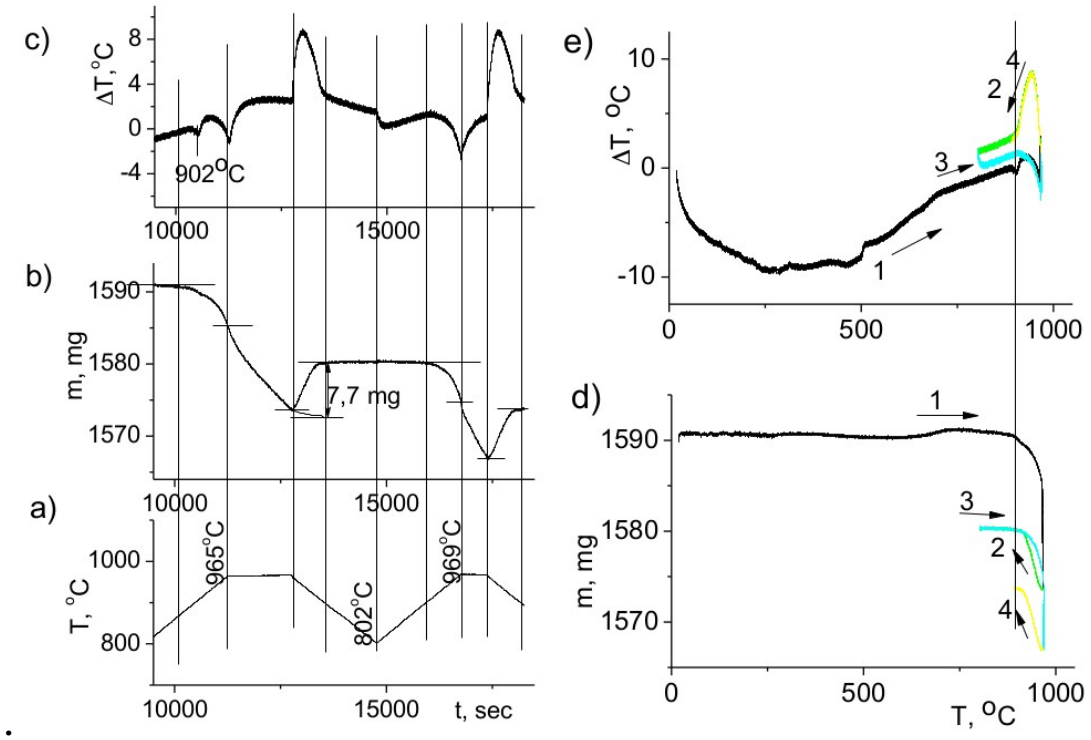

Figure SM1

References

[1] A. L. Spek, J. Appl. Cryst. **36**, 7 (2003).
[2] G. M. Sheldrick, *Acta Cryst.* ***A*64**, 112 (2008).
[3] International Tables for X-ray Crystallography, Vol. IV, (The Kynoch Press: Birmingham, England), 1974.
[4] J. Rodriguez-Carvajal, Physica B **192**, 55 (1993).
[5] T. B. Zunic and I. Vickovic, J. Appl. Cryst. **29**, 305 (1996).
[6] A. A. Bush, A. V. Titov, B. I. Al'shin, Yu. N. Venevtsev, Russ. J. Inorg. Chem. **22**, 1211 (1977).

3 additional tables

Table SM1. Results of the structural refinements of the $Pb_3Mn_7O_{15}$ samples using single crystal and powder XRD data and NPD data.

Experiment	**Crystal**	**Powder**			
	x-ray	**x-ray**	**neutron**		
T,K	295	295	295	70	1.8
a[Å]	9.979(1)	13.6127(2)	13.598(1)	13.546(1)	13.526(1)
b[Å]	9.979(1)	17.3437(4)	17.331(2)	17.262(2)	17.281(3)
c[Å]	13.598(3)	10.0226(2)	10.009(1)	9.926(1)	9.9219(8)
s.g.	***P63/mcm***	***Pnma***	***Pnma***	***Pnma***	***Pnma***
Pb_1					
x	0.38803(6)	0.2460(3)	0.2425(9)	0.2361(9)	0.2114(9)
y	0	0.4433(3)	0.4431(8)	0.4285(8)	0.4293(8)
z	0.25	0.4444(6)	0.4351(8)	0.4311(9)	0.4420(9)
$U_{aniso}/B[Å]^2$	0.0165(2)	0.83(1)	0.78(4)	0.55(4)	0.43(2)
Pb_2					
x	0	0.2562(3)	0.2586(8)	0.2321(8)	0.2386(8)
y	0.73502(6)	0.1196(3)	0.1163(9)	0.1115(7)	0.0969(9)
z	0.25	0.1123(6)	0.1139(8)	0.1012(9)	0.0733(9)
$B[Å]^2$	0.0179(2)	0.77(2)	0.67(3)	0.41(4)	0.39(1)
Pb_3					
x		0.7617(4)	0.7645(9)	0.7632(9)	0.7559(8)
y		0.25	0.25	0.25	0.25
z		0.9844(5)	0.9809(9)	0.9370(8)	0.0810(9)
$B[Å]^2$		0.65(2)	0.69(3)	0.51(4)	0.47(1)
Pb_4					
x		0.7536(5)	0.7414(8)	0.7392(8)	0.7787(8)
y		0.25	0.25	0.25	0.25
z		0.6410(6)	0.6688(9)	0.6354(8)	0.6067(9)
$B[Å]^2$		0.73(2)	0.75(3)	0.42(2)	0.36(2)
Mn_1					
x	0.33333	-0.0038(9)	-0.0173(9)	0.0023(9)	-0.0191(9)
y	0.6667	0.0797(8)	0.0873(8)	0.0518(7)	0.1105(9)
z	0.14819(12)	0.2567(9)	0.2428(9)	0.2386(8)	0.2274(8)
$B[Å]^2$	0.0081(4)	0.54(1)	0.64(2)	0.48(4)	0.58(2)
Mn_2					
x	0	0.0133(9)	0.0016(9)	0.0034(6)	0.0130(9)
y	0.5	0.3396(9)	0.3290(8)	0.3359(7)	0.3534(8)
z	0	0.5019(9)	0.4963(8)	0.5116(8)	0.5202(7)
$B[Å]^2$	0.0097(5)	0.48(1)	0.58(3)	0.49(2)	0.51(2)
Mn_3					
x	0.16822(8)	0.5046(8)	0.5199(9)	0.5061(9)	0.4917(7)
y	0.33645(16)	0.1668(9)	0.1631(8)	0.1700(8)	0.1769(8)
z	0	0.4966(8)	0.5207(9)	0.5234(9)	0.5215(6)
$B[Å]^2$	0.0103(3)	0.41(2)	0.66(3)	0.58(2)	0.58(2)

Mn_4					
x	0	0.1533(8)	0.1534(9)	0.1491(9)	0.1597(9)
y	0	0.4149(9)	0.4217(8)	0.4253(9)	0.3732(7)
z	0	0.7532(9)	0.7549(9)	0.6951(9)	0.7085(8)
$B[Å]^2$	0.0079(7)	0.38(3)	0.56(3)	0.46(2)	0.43(2)
Mn_5					
x		0.3558(8)	0.3405(8)	0.3618(7)	0.3980(9)
y		0.0851(9)	0.0817(8)	0.0746(9)	0.0662(8)
z		0.7472(9)	0.7032(9)	0.7378(9)	0.7308(8)
$B[Å]^2$		0.56(2)	0.66(2)	0.58(2)	0.54(2)
Mn_6					
x		0	0	0	0
y		0	0	0	0
z		0	0	0	0
$B[Å]^2$		0.52(2)	0.49(3)	0.46(2)	0.42(2)
Mn_7					
x		0	0	0	0
y		0	0	0	0
z		0.5	0.5	0.5	0.5
$B[Å]^2$		0.59(2)	0.47(2)	0.43(2)	0.39(2)
Mn_8					
x		0.5130(9)	0.4953(9)	0.4601(7)	0.4819(7)
y		0.25	0.25	0.25	0.25
z		0.7669(9)	0.7658(8)	0.7309(8)	0.7370(8)
$B[Å]^2$		0.42(2)	0.59(2)	0.58(2)	0.56(2)
Mn_9					
x		0.5051(9)	0.5024(8)	0.4824(8)	0.4579(8)
y		0.25	0.25	0.25	0.25
z		0.2638(8)	0.2575(9)	0.2705(9)	0.2913(9)
$B[Å]^2$		0.44(2)	0.54(2)	0.51(2)	0.47(2)
O_1					
x	0.1572(7)	-0.0664(9)	0.0781(9)	0.0142(8)	0.0667(7)
y	0.4876(6)	0.4340(8)	0.4881(9)	0.4717(7)	0.4838(9)
z	0.0794(4)	0.3672(9)	0.3173(9)	0.3170(8)	0.3254(9)
$B[Å]^2$	0.015(1)	0.81(3)	0.78(4)	0.67(4)	0.64(5)
O_2					
x	0	0.3667(9)	0.4169(9)	0.4088(8)	0.3979(9)
y	0.6683(8)	-0.0358(9)	0.0033(9)	0.0038(9)	0.0047(8)
z	0.0732(6)	0.2803(8)	0.3492(9)	0.3533(9)	0.3661(8)
$B[Å]^2$	0.016(1)	0.88(3)	0.78(6)	0.74(4)	0.72(6)
O_3					
x	0	0.2565(8)	0.2604(9)	0.2428(8)	0.2357(8)
y	0.1646(8)	0.5078(9)	0.5108(8)	0.5251(9)	0.5254(9)
z	0.0729(5)	0.1584(8)	0.1594(9)	0.1117(8)	0.1079(9)
$B[Å]^2$	0.016(2)	0.93(3)	0.67(5)	0.69(4)	0.67(5)
O_4					
x	0.1727(9)	0.8838(9)	0.9240(7)	0.9585(7)	0.9629(7)

y	0.6497(9)	0.3233(9)	0.3219(8)	0.3294(8)	0.3492(8)
z	0.25	0.7342(8)	0.6505(8)	0.5629(9)	0.6671(8)
$B[Å]^2$	0.0120(2)	0.97(4)	0.83(5)	0.81(5)	0.79(5)
O_5					
x		0.5911(8)	0.5828(7)	0.5944(8)	0.5985(7)
y		0.1801(9)	0.1706(9)	0.1860(9)	0.1930(9)
z		0.6515(9)	0.6648(9)	0.6763(9)	0.6740(9)
$B[Å]^2$		1.03(2)	0.79(4)	0.73(5)	0.68(4)
O_6					
x		0.9241(7)	0.9381(8)	0.9356(8)	0.9274(6)
y		0.25	0.25	0.25	0.25
z		0.4063(8)	0.4204(8)	0.4137(6)	0.4116(8)
$B[Å]^2$		0.86(3)	0.87(2)	0.76(2)	0.74(4)
O_7					
x		0.5868(9)	0.5812(8)	0.5766(8)	0.5786(8)
y		0.25	0.25	0.25	0.25
z		0.3805(8)	0.3863(9)	0.4068(7)	0.4682(7)
$B[Å]^2$		0.91(3)	0.94(3)	0.87(2)	0.82(3)
O_8					
x		0.4206(8)	0.4608(8)	0.4751(8)	0.4855(8)
y		0.25	0.25	0.25	0.25
z		0.5238(8)	0.6029(9)	0.6095(9)	0.6143(9)
$B[Å]^2$		0.96(3)	0.76(3)	0.72(3)	0.69(3)
O_9					
x		0.0917(9)	0.0735(7)	0.0732(7)	0.0867(7)
y		0.25	0.25	0.25	0.25
z		0.5614(9)	0.5486(9)	0.5349(9)	0.5173(7)
$B[Å]^2$		0.97(2)	0.86(4)	0.76(4)	0.73(4)
O_{10}					
x		0.9089(8)	0.9108(8)	0.9008(8)	0.9031(8)
y		0.5878(9)	0.5869(9)	0.5742(9)	0.5790(9)
z		0.4236(7)	0.4197(7)	0.3739(7)	0.3667(7)
$B[Å]^2$		0.85(2)	0.94(3)	0.94(3)	0.87(3)
O_{11}					
x		0.5737(9)	0.5591(7)	0.5766(7)	0.5702(7)
y		0.9134(9)	0.9275(8)	0.9241(8)	0.9077(8)
z		0.4208(9)	0.4129(7)	0.4173(7)	0.4189(7)
$B[Å]^2$		0.79(3)	0.67(3)	0.57(3)	0.54(3)
O_{12}					
x		0.0805(8)	0.0766(9)	0.0835(9)	0.0838(9)
y		0.3368(9)	0.3301(8)	0.3356(8)	0.3499(8)
z		0.3340(8)	0.3396(8)	0.3116(8)	0.2980(8)
$B[Å]^2$		0.83(3)	0.89(4)	0.82(4)	0.77(4)
O_{13}					
x		0.4237(7)	0.4343(8)	0.4263(9)	0.4104(7)
y		0.1612(9)	0.1698(9)	0.1644(8)	0.1705(9)

z		0.3261(8)	0.3117(8)	0.3008(9)	0.2855(8)
B[Å]^2		0.77(2)	0.74(3)	0.64(2)	0.61(3)
O_{14}					
x		0.2629(8)	0.2284(9)	0.2125(9)	0.2163(9)
y		0.6864(8)	0.6539(8)	0.6595(8)	0.6675(8)
z		0.1923(9)	0.1801(8)	0.1798(8)	0.1654(8)
B[Å]^2		0.88(2)	0.87(4)	0.81(4)	0.79(4)
O_{15}					
x		0.2423(9)	0.2591(7)	0.2396(7)	0.2096(7)
y		0.9100(8)	0.9311(8)	0.9465(8)	0.9668(8)
z		0.3813(9)	0.3943(7)	0.3915(7)	0.3857(7)
B[Å]^2		0.78(3)	0.79(3)	0.66(3)	0.63(3)
O_{16}					
x		0.0701(9)	0.9263(8)	0.9169(8)	0.9136(8)
y		0.4965(8)	0.4182(9)	0.4097(9)	0.4052(9)
z		0.3465(9)	0.4015(7)	0.4084(7)	0.4104(7)
B[Å]^2		0.87(2)	0.88(2)	0.81(2)	0.79(2)
O_{17}					
x		0.5836(9)	0.5795(8)	0.5715(8)	0.5687(8)
y		0.07876(8)	0.0860(9)	0.0764(9)	0.0628(9)
z		0.4240(7)	0.4286(9)	0.4226(9)	0.4201(9)
B[Å]^2		0.91(2)	0.94(3)	0.84(3)	0.81(3)
. R_p,%		1.96	3.14	3.61	4.30
. R_{wp},%		2.73	4.11	5.06	5.62
R_B(%)	3.96	4.03	4.13	4.24	3.06
R_{mag1}(%)		-	-		5.48
χ^2		1.46	1.65	1.43	1.29

Table SM2. Displacements of atoms during phase transformation from low temperature phase *Pnma* to high temperature phase *P63/mcm*. NOTE: u_x, u_y and u_z are given in relative units. |u| is the absolute distance given in Å

Atom	u_x	u_y	u_z	|u|
Pb1	0.002	-0.001	0.009	0.098
Pb2	0.006	0.002	0.010	0.131
Pb3	0.022	0.0000	0.006	0.2993
Pb4	-0.004	0.0000	0.012	0.134
Mn1	-0.002	0.0000	-0.007	0.075
Mn2	-0.007	0.001	-0.004	0.100
Mn3	-0.008	-0.0000	-0.009	0.144
Mn4	0.003	0.0000	0.009	0.099
Mn5	-0.005	0.001	0.007	0.104
Mn6	0.0000	0.0000	0.0000	0.0000
Mn7	0.0000	0.0000	0.0000	0.0000
Mn8	-0.001	0.0000	0.004	0.044
Mn9	0.013	0.0000	0.013	0.214
O1	-0.004	0.006	0.011	0.158
O2	0.003	0.005	-0.005	0.105
O3	0.011	0.002	0.011	0.190
O4	-0.010	-0.004	-0.001	0.155
O5	-0.018	-0.000	0.027	0.360
O6	-0.002	0.0000	-0.005	0.053
O7	-0.001	0.0000	0.014	0.145
O8	0.018	0.0000	0.000	0.248
O9	0.010	0.0000	-0.002	0.135
O10	-0.009	0.000	0.006	0.133
O11	0.001	0.005	-0.012	0.143
O12	-0.006	0.002	-0.004	0.099
O13	0.0000	0.001	0.018	0.183
O14	-0.015	-0.001	0.009	0.222
O15	0.007	-0.002	0.016	0.192
O16	-0.002	0.006	0.017	0.204
O17	0.006	0.004	0.003	0.108